Thermochimica Acta, 204 (1992) 69–77
Elsevier Science Publishers B.V., Amsterdam

Differential scanning calorimetry and thermostimulated current spectroscopy for the study of molecular orientation in polymers [1]

A. Bernès, D. Chatain and C. Lacabanne

Laboratoire de Physique des Solides (URA. CNRS / 74), Université Paul Sabatier, 31062 Toulouse Cédex (France)

(Received 16 January 1992)

Abstract

The influence of uniaxial and biaxial orientation on the transition/relaxation of poly(ethylene)terephthalate (PET) has been investigated. The transitions were studied by differential scanning calorimetry; the corresponding relaxations were studied by thermostimulated current (TSC) spectroscopy. At around 50°C, a particularly intense TCS peak was observed in the uniaxially oriented sample; this mode is a precursor of the glass transition T_g. The relaxation mode associated with the glass transition is observed at 82°C in unoriented PET, at 85°C in uniaxially oriented PET and at 100°C in biaxially oriented PET. An analysis of the fine structure has shown that it is made up of elementary processes that obey a compensation law: at the compensation temperature T_c, all the relaxation times become equivalent. It is important to note that for amorphous films (unoriented and uniaxially oriented) $T_c - T_g \approx 5°C$, whereas for the semi-crystalline film (biaxially oriented) $T_c - T_g \approx 15°C$. This result shows that crystallites are strongly coupled to the amorphous phase.

INTRODUCTION

The characterization of the amorphous phase of polymeric materials remains an unsolved problem. In fact, classical techniques such as differential scanning calorimetry (DSC) do not show the influence of molecular orientation on transition [1]. Therefore, thermostimulated current (TSC) spectroscopy has been applied to the study of the distribution of local order [2]. Poly(ethylene)terephthalate (PET) was chosen as the model material; the molecular orientation of the amorphous phase was obtained by varying the thermomechanical history. A thermostimulated current/relaxation map

---

Correspondence to: A. Bernès, Laboratoire de Physique des Solides (URA. CNRS/74), Université Paul Sabatier, 31062 Toulouse Cédex, France.

[1] This paper was presented during the 22nd meeting of the French Association of Calorimetry and Thermal Analysis (AFCAT) at Paris-XI–Châtenay-Malabry (27–29 May 1991).

analysis (TSC/RMA) spectrometer from Solomat was used for this investigation; differential scanning calorimetry was performed on a DSC II from Perkin-Elmer.

METHODS AND MATERIALS

Methods

In the DSC experiments, the sample was heated at a controlled rate of 20 K min^{-1} and the heat flow $\mathrm{d}H/\mathrm{d}T$ was recorded versus temperature T.

In the TSC experiments, the sample was first polarized by a static electric field E for a time and at a temperature that allows the dipolar species to orientate. When the polarization reached its equilibrium value, this configuration was frozen by decreasing the temperature. The electric field was then cut off and the sample connected to an electrometer. A controlled increase in temperature (7 K min^{-1}) then induced the recovery of the polarization. The depolarization current was measured by the electrometer, yielding the "dynamic conductivity" σ.

If P_i is the isothermal polarization varying exponentially with time, with a relaxation time τ_i

$$\frac{\mathrm{d}P_\mathrm{i}}{\mathrm{d}t} = -\frac{P_\mathrm{i}}{\tau_i} \tag{1}$$

where t is the time.

The relaxation time τ_i is given by

$$\tau_\mathrm{i} = \frac{P_\mathrm{i}}{\sigma E} \tag{2}$$

In polymers, the kinetics of the polarization is defined by a distribution of relaxation times

$$P = \sum_\mathrm{i} P_\mathrm{i} \tag{3}$$

The technique of fractional polarization [3] allows us to isolate P_i and so to determine the corresponding relaxation times τ_i.

In the vitreous state, the relaxation time is given by an Arrhenius equation

$$\tau = \tau_0 \exp\frac{\Delta H}{kT} \tag{4}$$

where τ_0 is the pre-exponential factor, ΔH is the activation enthalpy and k is the Boltzmann constant.

Experimental values deduced from eqn. (2) were plotted on an Arrhenius diagram, ln $\tau(1/T)$ and the relaxation map analysis (RMA) gave τ_0 and ΔH.

Around the glass transition temperature, the various relaxation times obey a compensation law

$$\tau = \tau_c \exp\left\{\frac{\Delta H}{k}\left(T^{-1} - T_c^{-1}\right)\right\} \tag{5}$$

where the compensation time τ_c and the compensation temperature T_c are constants. In that case, the relaxation times are only defined by one parameter, the activation enthalpy, because τ_0 is linked to ΔH by

$$\ln \tau_0 = \ln \tau_c - \frac{\Delta H}{kT_c} \tag{6}$$

So, on a compensation diagram where $\ln \tau_0$ is plotted versus ΔH, the experimental points following eqn. (5) define a "compensation line".

Materials

A serie of poly(ethylene)terephthalate (PET) films were prepared by Rhône-Poulenc for this study.

The biaxially oriented Terphane® (10 μm thick) has 39.5% crystallinity. It was produced in a two step-stretching process: the first in the travel direction, the second, of greater strain, in the transverse direction. The film was then heat-set at 180°C. The biaxially oriented films were compared with uniaxially oriented film (50 μm thick and 4% crystalline) obtained after the first process in the travel direction. The initial unoriented amorphous PET films (150 μm thick) were also studied as reference material.

EXPERIMENTAL RESULTS

Differential scanning calorimetry

DSC thermograms of PET films with various levels of molecular orientation are shown on Fig. 1.

The variation of the heat flow $\mathrm{d}H/\mathrm{d}t$ versus temperature T shows, for unoriented PET, the classical manifestation of the glass transition T_g around 75°C, the exothermic crystallization peak at 128°C and, finally, the endothermic melting peak at 252°C. As shown by curve b, the crystallization temperature is shifted by 40°C towards low temperatures upon uniaxial orientation. In the case of the biaxially oriented sample (curve c′), both the heat capacity step at T_g and the crystallization peak display a lower intensity than in the uniaxially oriented sample (curve b). This behavior can be explained by the high level of crystallinity (39.5%) of the sample.

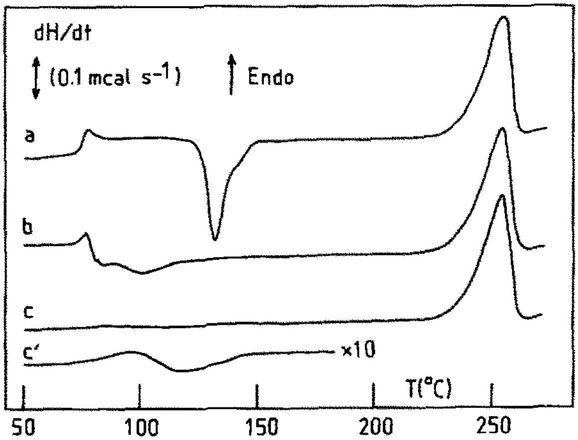

Fig. 1. DSC thermograms of: a, unoriented PET; b, uniaxially oriented PET; c, biaxially oriented PET; and c′, a magnification of a part of this thermogram.

Thermostimulated current spectroscopy

Complex TSC spectra

Complex TSC spectra of PET films with various levels of molecular orientation are shown on Fig. 2. The polarization field was respectively 2×10^6, 6×10^6 and 3×10^7 V m^{-1}; the polarization time was always 2 min and the polarization temperature was practically T_g as indicated by the arrows on Fig. 2. The TSC peak is situated respectively at 82 ± 0.5, 85 ± 0.5 and 100 ± 0.5°C for the unoriented, uniaxially and biaxially oriented PET. For clarity, the peak corresponding to biaxially oriented PET has been multiplied by 10.

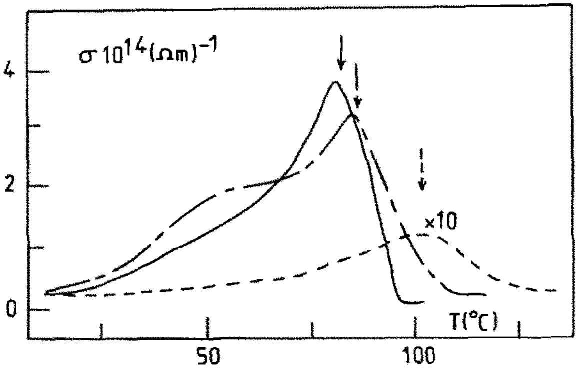

Fig. 2. Complex TSC spectra of: (———), unoriented PET; (— – —), uniaxially oriented PET; and (— — —), biaxially oriented PET.

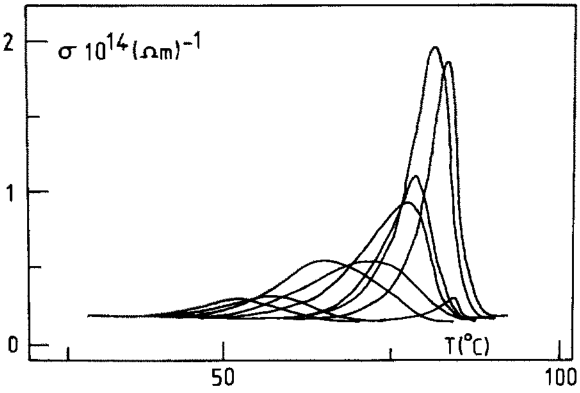

Fig. 3. Elementary TSC spectra of unoriented PET recorded after polarization at T_p performed in the 40–80°C range with 5°C steps.

Because these peaks are situated around the glass transition temperature, they have been attributed to the dielectric manifestation of the glass transition. This hypothesis is consistent with the strong decrease of its magnitude in biaxially oriented PET inherent with its relatively high crystallinity. Around 50°C, it is interesting to note the existence of a sub-T_g relaxation mode.

Relaxation map analysis

Using fractional polarizations, the complex TSC spectra were resolved into elementary processes. The principle of the fractional polarization procedure is as follows. The sample is subjected to the electric field for a time (2 min) at a temperature (T_p) that allows the polarization of dipolar entities with relaxation times $\tau \leq \tau_i$. Then the temperature is decreased by

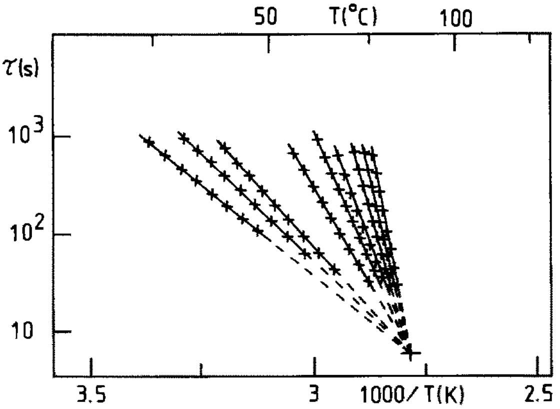

Fig. 4. Arrhenius diagram of dielectric relaxation times of unoriented PET.

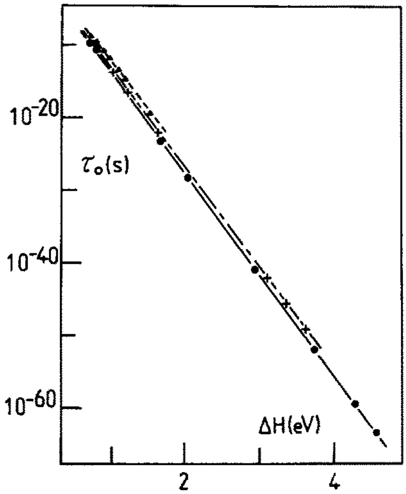

Fig. 5. Compensation diagram of: ●, unoriented PET; +, uniaxially oriented PET; and ▲, biaxially oriented PET.

5°C and the field is cut off. The temperature is maintained constant for another 2 min to allow for disorientation of the dipoles having a relaxation time $\tau < \tau_i$. This configuration is frozen and a classical TSC scan shows the response of a monokinetic process giving an elementary TSC spectrum.

Figure 3 shows, as an example, the elementary TSC spectra isolated in unoriented PET. The electric field is the same as for the complex spectrum and the "temperature window" was 5°C. The value of T_p was varied in steps of 5°C in the range $40°C \leq T_p \leq 80°C$. It is interesting to note that the temperatures of the TSC maxima are shifted, indicating the existence of a distribution of relaxation times. Each elementary spectrum was analysed and the temperature dependence of the corresponding relaxation times were deduced from eqn. (2). Then, the experimental points were plotted on an Arrhenius diagram (Fig. 4). By extrapolation, we see that all the $\tau(T)$ variations converge at a given temperature: they are obeying the compensation equation (eqn. (5)). Thus, a compensation line is defined on the compensation diagram (Fig. 5). We also report the experimental points corresponding to the uniaxially oriented PET and to the biaxially oriented

TABLE 1

Values of the compensation parameters

Sample	T_c (°C)	τ_c (s)
Unoriented PET	87 ± 1	6.2 ± 0.5
Uniaxially oriented PET	91 ± 1	17 ± 0.5
Biaxially oriented PET	115 ± 1	10 ± 0.5

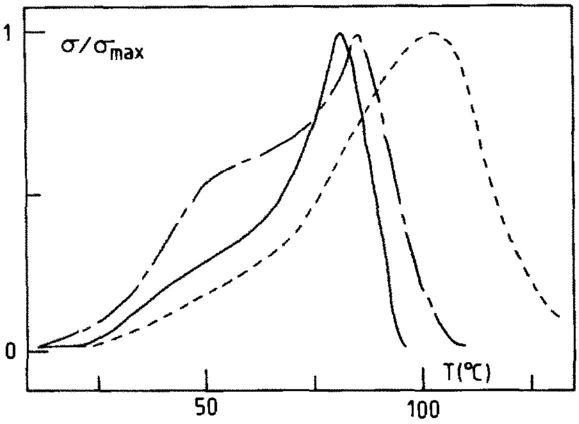

Fig. 6. Normalized complex TSC of: (———), unoriented PET; (— – —), uniaxially oriented PET; and (— — —), biaxially oriented PET.

PET. The values of the compensation parameters obtained for the three samples are listed in Table 1.

DISCUSSION

A comparison of the transition spectrum with the dielectric relaxation spectrum in various samples of PET has shown that the glass transition and the corresponding relaxation are very sensitive to molecular orientation.

*Sub-*Tg *relaxation mode*

Around 50°C, a sub-T_g relaxation mode is observed in all PET samples. Figure 2 shows the variation of the magnitude of this mode as a function of molecular orientation. To facilitate this comparison, the TSC spectra recorded after polarization at T_g have been normalized; they are represented in Fig. 6. It is evident that the magnitude of the sub-T_g mode is greatest in the uniaxially oriented PET.

In fact, we have other evidence of low-temperature molecular mobility in this sample: the DSC thermograms (Fig. 1) reveal that the crystallization phenomenon observed at 128°C in unoriented PET is shifted to 80°C in uniaxially oriented PET. This evolution reveals a significant increase of molecular mobility in the vitreous region below T_g. This result has been confirmed by other experimental evidence from dilatometry and enthalpic measurements [4]. Therefore, the magnitude of the sub-T_g mode can be used for evaluating the inhomogeneity of a polymer.

T_g *relaxation mode*

The TSC spectra of PET films (Fig. 2) show that the amorphous phase is modified upon molecular orientation. Indeed, this amorphous phase is characterized by a distribution of relaxation times obeying a compensation law. The different processes are dependent: at the compensation temperature there will be a kind of resonance. For unoriented PET and uniaxially oriented PET, $T_c - T_g \approx 5$°C, while for biaxially oriented PET, $T_c - T_g \approx 15$°C. It is interesting to note that this latter value is consistent with those obtained for other semi-crystalline polymers such as polypropylene ($T_c - T_g = 33 \pm 1.5$°C [5] and polyamide ($T_c - T_g = 28 \pm 1.5$°C) [6] where the crystallinity rate is about 50%. Therefore, when the crystallinity rate is small, the amorphous and crystalline phases are not coupled; when it reaches around 40%, the amorphous and crystalline phases become coupled.

To explain this, the hypothesis of an intermediate biphasic structure of the amorphous phase has been proposed. In addition to the "true" amorphous phase, an "ordered" amorphous phase with short-range nematic order [7,8] would be induced in uniaxially oriented PET. This would be the precursor of the crystallites in biaxially oriented PET. The crystallization procedure would be responsible for the coupling between the amorphous and crystalline phases.

As shown in Fig. 5, the magnitude of the compensation phenomenon is considerably reduced by crystallinity. According to the model of Hoffman et al. [9], the increase in activation enthalpy reflects the increase in the length of the mobile sequences. In uniaxially oriented PET, this length would be reduced by the ordered amorphous phases; in biaxially oriented PET, it would be highly restricted by the crystallites.

CONCLUSIONS

A comparative study of the transitions and dielectric relaxations of PET has been performed by DSC and TSC in analogous experimental conditions. In unoriented PET, a "true" amorphous phase with delocalized cooperative movements has been characterized. Upon uniaxial orientation, an "ordered" amorphous phase appears. After biaxial orientation, this is transformed into crystalline domains. At the same time, a restriction of the length of the mobile sequences in the true amorphous phase is observed.

REFERENCES

1 R. Hagege, C. Mamy and C. Thiroine, Makromol. Chem., 179 (1978) 1069-1081.

2 A. Bernès, R.F. Boyer, D. Chatain, C. Lacabanne and J.P. Ibar, in S.E. Keinath, R.L. Miller and J.K. Rieke (Eds.), Order in the Amorphous State of Polymers, Plenum Press, New York, 1987, pp. 305-326.

3 D. Chatain, P. Gautier and C. Lacabanne, J. Polym. Sci. Phys. Ed., 11 (1973) 1631-1640.

4 V. Busico, P. Corradini and F. Riva, Makromol. Chem. Rapid Commun., 1 (1980) 423-426.

5 M. Jarrigeon, B. Chabert, D. Chatain, C. Lacabanne and G. Nemoz, J. Macromol. Sci. Phys. B, 17 (1980) 1–24.
6 M. Stefenel, Thèse 3ème Cycle, University Paul Sabatier, Toulouse, 1984.
7 P. Bouriot, J. Jacquemart and M. Sottom, Bull. Sci. Inst. Text. Fr., 6 (1977) 9–18.
8 W.L. Lindner, Polymer, 14 (1973) 9–15.
9 J.D. Hoffman, G. Williams and E. Passaglia, J. Polym. Sci. C, 14 (1966) 173–235.